Mobility-Aware Predictive Beamforming Design in Sensing-assisted SWIPT Systems

Junyuan Fan, *Student Member, IEEE*, Yayun Wei, Jie Tang, *Senior Member, IEEE*, Tianyi Liu, Kai-Kit Wong, *Fellow, IEEE*

***Abstract*—Thanks to the advanced beamforming techniques, the efficiency of wireless power transfer (WPT) in simultaneous wireless information and power transfer (SWIPT) systems has been considerably improved. However, the frequent channel state information (CSI) feedback will decrease in the actual harvested energy once the receiver is out of the stable quiescent state. To address this challenge, we envision a novel sensing-assisted SWIPT system where a hybrid access point (HAP) serves multiple communication users (IUs) and a mobile energy user (MEU). Especially, an extended Kalman filtering (EKF)-based tracking framework is proposed to track the dynamic MEU by exploiting echo signals. A real-time beamforming design problem is then formulated and efficiently solved to maximize the real-time WPT efficiency. Simulation results validate that the proposed scheme can accurately track and achieve higher WPT efficiency than benchmark schemes.**

***Index Terms*—Simultaneous wireless information and power transfer, integrated sensing and communication (ISAC), beamforming design, optimization.**

I. Introduction

With the advent of the "Ubiquitous Internet of Things (IoT)" concept, numerous emerging IoT application scenarios, such as unmanned factories and smart homes, have begun to capture public attention [1]. These scenarios necessitate many low-power sensors to enable sustainable environmental monitoring, data collection, and intelligent control. As a promising technology, SWIPT has emerged as one of the most promising solutions, enabling base stations (BS) or access points (APs) to provide information transmission and wireless charging concurrently. Therefore, sensors can gain energy from remote sources via radio frequency (RF) to achieve true wireless power supply, thus opening new avenues for the widespread deployment and sustainable operation of IoT devices [2]. Recently, significant attention has been devoted to beamforming design in multi-antenna SWIPT systems, aiming to maximize energy harvesting efficiency through well-designed precoding vectors [3]–[5]. With emerging low-power applications such as asset tracking and small wearable devices, dynamic WPT is becoming a promising technological direction [6]. However, the transmitter must continuously acquire CSI to enable beamforming-based transmission. This process activates energy-intensive hardware at the receiver, such as processing units and power amplifiers, which can reduce the actual harvested energy and present a notable challenge. Balancing the additional resource consumption and energy loss caused by CSI acquisition with WPT efficiency thus emerges as a critical research direction.

Integrated Sensing and Communication (ISAC), which enables BS to characterize environment through wireless sensing, is emerging as a key technology in 6G networks. Specifically, recent studies have demonstrated the potential of radar localizing to enhance high dynamic communication performance [7]. The approach that leverages sensing capabilities to improve the efficiency and reliability of wireless systems is also commonly referred to as sensing-assisted ISAC. Subsequently, the integration of sensing-assisted ISAC with various cutting-edge communication technologies were studied. In [8], the application of Reconfigurable Intelligent Surface (RIS)-aided ISAC in vehicular networks was studied, utilizing sensing information from the previous time slot to maximize communication performance. In [9], an ISAC system integrating air-space-ground communication with UAV assistance was proposed, optimizing the system energy efficiency. In addition to these efforts where user localization is sensed, some works addressed secure communication by leveraging sensing to detect eavesdroppers [10], [11].

With the increasing diversification of BS functionalities, integrating sensing, wireless power transfer, and communication capabilities, i.e., combining ISAC with SWIPT, has emerged as a novel research direction and gained considerable attention [12]–[15]. In [12], a novel multiple-input multiple-output (MIMO) system that integrates sensing, communication, and power transfer was investigated to reveal the performance trade-offs and Pareto boundaries through transmit covariance optimization. Additionally, a multi-user MIMO system for integrated sensing, communication, and power transfer (ISCPT) was proposed in [13], optimizing beamforming and power allocation to balance performance among multiple users. Furthermore, a RIS-aided ISCPT system was investigated in [14], where the received energy was maximized by jointly optimizing transmit beamforming at both the BS and RIS side. However, current works on the integration of

This paper was supported in part by the National Natural Science Foundation of China under Grant 62222105. (Corresponding authors: Jie Tang)

J. Fan, Y. Wei and J. Tang are with the School of Electronic and Information Engineering, South China University of Technology, Guangzhou 510640, China (e-mail: eefanjy@mail.scut.edu.cn, weiyayungd@163.com, eejtang@scut.edu.cn).

T. Liu is with the China United Network Communications Group Co., Ltd., Beijing 100031, China and he also with the School of Artificial Intelligence, Beijing University of Posts and Telecommunications, Beijing 100876, China (e-mail: liuty101@chinaunicom.cn)

K.K. Wong is with Department of Electronic and Electrical Engineering, University College London, London WC1E 6BT, United Kingdom. He is also with Yonsei Frontier Lab, Yonsei University, Seoul, Korea (e-mail: kai-kit.wong@ucl.ac.uk).

Manuscript received December 19, 2024

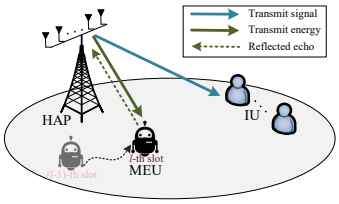

Fig. 1: Illustration of a sensing-assisted SWIPT system.

ISAC and SWIPT primarily treat the sensing function as a separate service. Moreover, existing studies focus primarily on static energy users, paying limited attention to beamforming strategies for dynamic low-power terminals. Given that MEUs require sensing information akin to mobile communication users, leveraging sensing capabilities to enhance SWIPT systems for simultaneous communication, power transfer, and tracking has become a promising research direction. In [15], although a system combining ISAC and SWIPT with mobile energy terminals was studied, the sensing and charging services were realized through time-division, which requires more system resources. To the best of our knowledge, utilizing radar sensing in SWIPT systems with moving energy devices to realize tracking, energy harvesting and communication quality remains an open problem.

To effectively address the aforementioned challenges, this letter introduces a novel framework that leverages ISAC tracking to realize efficient WPT, constructing an online beamforming design problem. The contributions of this work are summarized as follows: (1) A novel sensing-assisted SWIPT system is developed, where reflected signal echoes are utilized to track MEUs and facilitate efficient WPT. (2) An online beamforming optimization framework is formulated, aiming to maximize energy transfer efficiency while considering specific tracking and transmission requirements. (3) The proposed approach eliminates the need for uplink feedback from energy receivers, thereby reducing system overhead and enhancing energy efficiency. The effectiveness of the proposed framework is verified through simulation results, which demonstrate enhanced energy transfer efficiency and improved overall system performance compared to benchmark schemes.

II. SYSTEM MODEL

As shown in Fig. 1, we consider a novel sensing-assisted SWIPT system where a multi-antenna HAP transmits communication signals to K single-antenna IUs (indexed by $k \in \mathcal{K} = \{1, \ldots, K\}$). Meanwhile, the HAP provides wireless charging for a point-like MEU that moves within a certain reachable range. The HAP is equipped with uniform linear arrays (ULAs) with M_t transmit antennas and M_r receive antennas. The MEU is equipped with an RF energy harvesting module and moves along a predetermined route that is unknown to HAP within a total task time T. [1] The HAP and IUs are fixed at $\mathbf{q} = [q_0^x, q_0^y]^T$, $\mathbf{q}_k^{\mathrm{IU}} = [q_k^x, q_k^y]^T$ respectively. Without loss of generality, we assume $K < M_t$. In our proposed scheme, service time T is divided into L frames with equal length δ, i.e. $T = L\delta$. [2]

A. Channel Model

The HAP-IU channel $\mathbf{h}_k$ and time-varying HAP-MEU channel at l-th frame $\mathbf{g}_{E,l}$, are respectively given by

$$\mathbf{h}_k = \sqrt{\beta_0 d_k^{-2}}\mathbf{a}_{M_t}^T(\varphi_k) \tag{1}$$

$$\mathbf{g}_{E,l}(d_{E,l}, \varphi_{E,l}) = \sqrt{\beta_0 d_{E,l}^{-2}}\mathbf{a}_{M_t}^T(\varphi_{E,l}) \tag{2}$$

where β_0 denotes the channel gain at a reference distance, d_k and $d_{E,l}$ denote the Euclidean distances between HAP and k-th IU, HAP and MEU, respectively. As this study represents the first exploration of beamforming design in dynamic SWIPT systems, we assume all links are primarily dominated by line-of-sight (LoS) conditions to simplify the analysis [16]. [3] Therefore, the transmit array steering vector is modeled as $\mathbf{a}_{M_t}(\phi) = \left(1, e^{-j\pi\cos\phi}, ..., e^{-j\pi(M_t-1)\cos\phi}\right)$, where $\phi = \{\varphi_k, \varphi_{E,l}\}$ denotes the azimuth angle.

B. Communication & Powering Model

At the l-th frame, the downlink transmitted signal by HAP is denoted by $x_l(t)$, which can be expressed as

$$x_l(t) = \mathbf{v}_l s_0^{\mathrm{E}}(t) + \sum_{k\in K}\mathbf{w}_{k,l}s_k^{\mathrm{I}}(t) \tag{3}$$

where $\mathbf{w}_{k,l}$ and $\mathbf{v}_l$ denote the beamforming vectors for k-th IU and MEU, respectively. The information-bearing signals s_k^{I} are assumed to be $s_k^{\mathrm{I}} \sim \mathcal{CN}(0,1), \forall k$, while the dedicated energy-carrying signal s_0 are generated from an arbitrary distribution with $\mathbb{E}\left\{|s_0|^2\right\} = 1$, since it does not convey any communication information. The total transmit power should not exceed the power budget of the system $P_{\max}$, i.e. $P_{t,l} = \sum_{k\in K}\|\mathbf{w}_{k,l}\|^2 + \|\mathbf{v}_l\|^2 \le P_{\max}$. The received signal at IU k in lth frame is given by

$$y_{k,l}^{\mathrm{I}}(t) = \sum_{j\in K}\mathbf{h}_k\mathbf{w}_{k,l}s_j^{\mathrm{I}}(t) + \mathbf{h}_k\mathbf{v}_l s_0^{\mathrm{E}}(t) + z_k(t) \tag{4}$$

where $z_k \sim \mathcal{CN}(0, {\sigma_k}^2)$ is the Additive White Gaussian noise (AWGN) noise. The corresponding received SINR of IU k is then expressed as

$$\gamma_k(\mathbf{w}_{k,l}) = \frac{|\mathbf{h}_k\mathbf{w}_{k,l}|^2}{\sum\limits_{j\neq k, j\in K}|\mathbf{h}_k\mathbf{w}_{k,l}|^2 + \sigma_k^2} \tag{5}$$

In terms of energy charging for MEUs, the instantaneous received RF power at the l-th frame can be formulated as

$$E_l(\mathbf{w}_{k,l}, \mathbf{v}_l) = \mu\mathbf{g}_{E,l}\left(\mathbf{v}_l\mathbf{v}_l^H + \sum_{k\in K}\mathbf{w}_{k,l}\mathbf{w}_{k,l}^H\right)\mathbf{g}_{E,l}^H \tag{6}$$

where $\mu \in (0,1)$ is the system energy conversion constant.

The WPT efficiency of the system is defined as the ratio of harvested power E_l by the MEU and the total power consumption $P_{tot,l}$ at the HAP in frame l, given by

$$\eta_{\mathrm{WPT},l} = \frac{E_l(\mathbf{w}_{k,l}, \mathbf{v}_l)}{P_{tot,l}(\mathbf{w}_{k,l}, \mathbf{v}_l)} \tag{7}$$

[1] This could arise due to practical constraints such as limited communication, or security and privacy concerns restricting the sharing of route details with HAP. Consequently, the HAP works without prior knowledge of the MEU's trajectory.

[2] We assume that the computation time consuming can be ignored with advanced signal processing techniques.

[3] Short-range transmission is considered in the proposed system due to the actual implementation of WPT, thus the strong Los-dominated channel assumption is reasonable.

where $P_{tot,l} = \varsigma P_{t,l} + P_C$, ς is the power amplifier efficiency and P_C is the circuit power consumption.

C. Radar Sensing & EKF Tracking Model

The HAP is assumed to operate in full-duplex and while transmitting downlink SWIPT signal, concurrent sensing is carried out based on MEU echos, expressed as [3]

$$r_l(t) = e^{j2\pi\upsilon_l t}\mathbf{g}_{r,l}x(t-\tau_l) + z_{r,l}(t) \tag{8}$$

where υ_l, τ_l, $z_{r,l}$ denote the echo's Doppler shift, delay and receiver noise, respectively. The round-trip channel is modeled as $\mathbf{g}_{r,l} = \frac{\chi\beta_0}{2d_l^{\text{MEU}}}\mathrm{b}_{M_r}(\varphi_l)\,\mathrm{a}_{M_t}^T(\varphi_l)$, where $\chi = \sqrt{\kappa(4\pi d_l^2)^{-1}}$ is the reflection coefficient and κ is radar cross section (RCS). Particularly, let vector $\mathbf{O}_l = [\varphi_l, \tau_l, \upsilon_l]^T$ represents the estimated parameters obtained by signal process methods such as match filtering [17]. Then the corresponding estimation variances, $\sigma_{\varphi,l}^2$, $\sigma_{\tau,l}^2$, $\sigma_{v,l}^2$, are inversely proportional to the received SNR, which can be given by

$$\Gamma_l(\mathbf{v}_l) = \frac{\kappa\beta_0^2\alpha_{\text{MF}}M_r\left|\mathrm{a}_{M_t}^T(\varphi_l)\,\mathbf{v}_l\right|^2}{16\pi d_{E,l}^4\sigma_{\text{R}}^2} \tag{9}$$

where α_{MF} is the MF gain and σ_{R}^2 is the HAP receiver noise.

The MEU time-varying motion parameters are defined as $\mathbf{X}_l = \left[\mathbf{q}_l^{\text{E}}, \mathbf{u}_l^{\text{E}}\right]^T$, where $\mathbf{q}_l^{\text{E}} = [q_l^x, q_l^y]^T, \mathbf{u}_l^{\text{E}} = [u_l^{\text{x}}, u_l^y]^T$ denote the location and velocity of MEU, respectively. Thus, the model of state transition from the current frame to the next frame is given by $\mathbf{X}_l = \mathbf{A}\cdot\mathbf{X}_{l-1} + \mathbf{z}_{pl}$, where $\mathbf{A} = [\mathbf{I}_{2\times2}, \delta\cdot\mathbf{I}_{2\times2}; \mathbf{0}_{2\times2}, \mathbf{I}_{2\times2}]$ denotes the linear state transition matrix and $\mathbf{z}_{pl}$ is the process noise vector with $\mathbf{z}_{pl} \sim CN(0, \mathbf{Q}_Z)$.

An EKF-based framework is employed to achieve closed-loop target tracking, as EKF filtering efficiently fuses multiple data sources to minimize state estimation uncertainty and error [18]. The radar observation model which characterizes the relationship between estimated parameters and motion parameters is given by $\mathbf{O}_l = f(\mathbf{X}_l) + \mathbf{z}_{sl}$, where $f(\cdot)$ is the non-linear observation operator, given by $f(\mathbf{X}_l) = \left[\arctan\frac{q_l^y}{q_l^x}, \frac{2\sqrt{\left(q_l^x\right)^2+\left(q_l^y\right)^2}}{c}, \frac{2f_c u_l^x q_l^x}{c\sqrt{\left(q_l^x\right)^2+\left(q_l^y\right)^2}}\right]^T$ and $\mathbf{z}_{sl}$ is the radar estimation noise with $\mathbf{z}_{sl} \sim CN(0, \mathbf{Q}_S)$, where $\mathbf{Q}_S = \text{diag}(\sigma_{\varphi l}^2, \sigma_{\tau l}^2, \sigma_{vl}^2)$. Recall the inverse relationship between noise variance and the received SNR, we further reformulate the estimation variances as $\sigma_{\Omega_i}^2 = \frac{a_{\Omega_i}}{\Gamma_l}$, where $i \triangleq \left\{\sigma_\varphi^2, \sigma_\tau^2, \sigma_v^2\right\}$, and a_{Ω_i} is determined by system configuration. The estimation covariance is then recast as $\mathbf{Q}_S = {\Gamma_l}^{-1}(\mathbf{v}_l)\,\text{diag}\left(a_{\Omega\sigma_\varphi^2}, a_{\Omega\sigma_\tau^2}, a_{\Omega\sigma_v^2}\right)$.

The fusion steps of the estimated and predicted data are as follows: At the beginning of each frame, state prediction is performed as $\hat{\mathbf{X}}_{l|l-1} = \mathbf{A}\tilde{\mathbf{X}}_{l-1}$, with prediction covariance $\hat{\mathbf{M}}_{l|l-1} = \mathbf{A}\mathbf{M}_{l-1}\mathbf{A}^H + \mathbf{Q}_Z$. The Kalman filter gain is then calculated as $\mathbf{K}_l = \hat{\mathbf{M}}_{l|l-1}\mathbf{F}_l^H\left(\mathbf{F}_l\hat{\mathbf{M}}_{l|l-1}\mathbf{F}_n^H + \mathbf{Q}_S\right)^{-1}$, where $\mathbf{F}_l = \frac{\partial f}{\partial x}\Big|_{x=\hat{\mathbf{X}}_{l|l-1}}$ denotes the Jacobian matrix of the observation model. Therefore, the updated motion state and covariance matrix are, respectively, formulated as

$$\tilde{\mathbf{X}}_l = \hat{\mathbf{X}}_{l|l-1} + \mathbf{K}_l\left(\mathbf{O}_l - f\left(\hat{\mathbf{X}}_{l|l-1}\right)\right) \tag{10}$$

$$\mathbf{M}_l = (\mathbf{I}_4 - \mathbf{K}_l\mathbf{F}_l)\cdot\hat{\mathbf{M}}_{l|l-1} \tag{11}$$

By iteratively performing the above steps and updating $\tilde{\mathbf{X}}_l$ and $\mathbf{M}_l$, HAP can realize the positioning and tracking of MEU, which we call the sensing-assisted SWIPT method. In the next section, we will focus on the real-time beamforming design based on tracked vector $\tilde{\mathbf{X}}_l$ during each frame iteration, and guarantee reliable tracking of the MEU.

III. Dynamic Wireless Powering via Online Beamforming Design

A. Problem Formulation

In this work, our goal is to maximize the real-time WPT efficiency for each frame via online optimization of the transmit beamforming, subject to system quality-of-service(QoS) requirements, which includes the individual SINR demands at each IU, the energy harvesting and sensing QoS at MEU. Note that the trace of tracking covariance matrix represents the posterior mean squared error (MSE) for MEU tracking, thus we define the instantaneous tracking performance as $\mathcal{S} = \text{tr}(\mathbf{M}_l)$, which is implicitly a function of beamforming vector $\mathbf{v}$. For notation convenience, the frame index l is omitted in this section. The corresponding beamforming problem is formulated as follows,

$$\text{(P0)}\max_{\mathbf{w}_k,\mathbf{v}} \quad \eta_{\text{WPT}}(\mathbf{w}_k,\mathbf{v}) = \frac{\hat{E}(\mathbf{w}_k,\mathbf{v})}{P_{tot}(\mathbf{w}_k,\mathbf{v})} \tag{12a}$$

$$\text{s.t.} \quad P(\mathbf{w}_k,\mathbf{v}) \le P_{\max}, \tag{12b}$$

$$\text{SINR}_k(\mathbf{w}_k) \ge \gamma_{\min}, \tag{12c}$$

$$\hat{E}(\mathbf{w}_k,\mathbf{v}) \ge e_{\min}, \tag{12d}$$

$$\mathcal{S}(\mathbf{v}) \le C_{\max}. \tag{12e}$$

where (12b) denotes the transmit power budget, (12c) guarantees the minimum SINR for IU. For the harvested energy constraint (12d), $\hat{E}$ denotes the prediction energy at the time of beamforming design and $e_{\text{min,l}}$ is the minimal power demand at lth frame. The pre-defined parameter $C_{\max}$ in (12e) denotes the upper limit of tracking performance.

B. Proposed Solution

Note that problem $P0$ is challenging to solve, due to the fractional objective function and the non-convex constraints. Thus in this subsection, we present the following algorithm to tackle with the non-convexity and intractability.

To address the non-convex objective function, we apply nonlinear fractional programming based on the Dinkelbach method [19] where the corresponding subtractive form of objective function (12a) is given by $\hat{E}(\mathbf{w}_k,\mathbf{v}) - \eta P_{\text{tot}}(\mathbf{w}_k,\mathbf{v})$. It is well-proved that with the unique zero η^*, we can recast problem $P0$ into the following equivalent form

$$\text{(P1)}\max_{\mathbf{w}_k,\mathbf{v}} \quad \hat{E}(\mathbf{w}_k,\mathbf{v}) - \eta P_{\text{tot}}(\mathbf{w}_k,\mathbf{v}) \tag{13a}$$

$$\text{s.t.} \quad (12\text{b}),(12\text{c}),(12\text{d}),(12\text{e}). \tag{13b}$$

To solve the problem efficiently, we then introduce auxiliary variables $\mathbf{W} = \mathbf{w}\mathbf{w}^H$ and $\mathbf{V} = \mathbf{v}\mathbf{v}^H$, with constraints $\mathbf{W}_k \ge$

[3]signals reflected by other scatters are omitted here as they can be effectively suppressed by existing clutter suppression techniques.

Algorithm 1 The Proposed Overall Algorithm

Require: Initial point $\tilde{\mathbf{X}}_0$ and $\mathbf{M}_0$.

1: **for** $l = 1, 2, 3, \ldots$ **do**
2: Compute prediction state $\hat{\mathbf{X}}_{l|l-1}$ and $\hat{\mathbf{M}}_{l|l-1}$.
3: Compute Jacobian matrix $\mathbf{F}_l = \frac{\partial f}{\partial x}\Big|_{x=\hat{\mathbf{X}}_{l|l-1}}$.
4: Solve the optimization problem (14) to obtain the optimal predictive beamforming vector $\left(\mathbf{w}_{k,l}^*, \mathbf{v}_l^*\right)$ and performs SWIPT and echo sensing.
5: Compute Kalman gain $\mathbf{K}_l$ with $\mathbf{Q}_{\mathrm{s}}\left(\mathbf{V}_l^*\right)$.
6: Update state and covariance $\tilde{\mathbf{X}}_l$ and $\mathbf{M}_l$.
7: **return** tracking results $\tilde{\mathbf{X}}_l$ and $\mathbf{M}_l$ for all l.

$0, \mathbf{V} \geq 0$, $\mathrm{rank}\left(\mathbf{W}_k\right) = 1$ and $\mathrm{rank}\left(\mathbf{V}\right) = 1$. Hence, the aforementioned optimization problem is reformulated as

$$\text{(P1)} \max_{\mathbf{W}_k, \mathbf{V}} \quad \hat{E}\left(\mathbf{W}_k, \mathbf{V}\right) - \eta P_{\mathrm{tot}}\left(\mathbf{W}_k, \mathbf{V}\right) \tag{14a}$$

$$\text{s.t.} \quad \sum_{k \in K} \mathrm{tr}\left(\mathbf{W}_k\right) + \mathrm{tr}\left(\mathbf{V}\right) \leq P_{\max}, \tag{14b}$$

$$\frac{\mathrm{tr}\left(\mathbf{h}_k^H \mathbf{h}_k \mathbf{W}_k\right)}{\mathrm{tr}\left(\mathbf{h}_k^H \mathbf{h}_k \sum\limits_{j \neq k, j \in K} \mathbf{W}_j\right) + \sigma_k^2} \geq \gamma_{\min}, \tag{14c}$$

$$\mu\left(\mathrm{tr}\left(\hat{\mathbf{g}}^H \hat{\mathbf{g}} \mathbf{V}\right) + \sum_{k \in K} \mathrm{tr}\left(\hat{\mathbf{g}}^H \hat{\mathbf{g}} \mathbf{W}_k\right)\right) \geq e_{\min}, \tag{14d}$$

$$\mathrm{tr}\left(\mathbf{M}_l\right) \leq C_{\max}, \tag{14e}$$

$$\mathbf{W}_k \geq 0, \quad \mathbf{V} \geq 0, \tag{14f}$$

$$\mathrm{rank}\left(\mathbf{W}_k\right) = 1, \quad \mathrm{rank}\left(\mathbf{V}\right) = 1, \forall k. \tag{14g}$$

where $\hat{\mathbf{g}}$ is the prediction BS-MEU channel. Problem (14), however, is still non-convex owing to the rank-one constraints. Fortunately, this nonconvexity can be addressed by the classical SDR [20] approach. Therefore, by dropping constraints $(14\mathrm{g})$, problem P1 is converted into an SDR programming, which can be efficiently solved by standard solvers such as CVX [21]. Note that the feasible rank-one solution of the original problem can be obtained by eigenvalue decomposition or Gaussian randomization procedure.

To sum up, by iteratively predicting and tracking, the HAP can simultaneously sense targets, transmit energy and signals at a low resource cost. The details for the proposed online beamforming algorithm are summarized in **Algorithm** 1.

IV. Simulation Results

In this section, numerical results are presented to demonstrate the effectiveness of our proposed real-time beamforming design. We set the HAP at (0,0) and equipped with $M_t = 8, M_r = 2$ antennas to serve $K = 3$ single-antenna IUs and one MEU. The locations of IUs are (2,6)m, (6,1)m and (4,-6)m, the initial location of MEU is (-8,10)m. The system operates at 5.5 GHz [22] and reference channel power gain is calculated by free space propagation model. The remaining simulation parameters are listed as follows [10] [23]: $\gamma_{\min} = 5$dB, $e_{\min} = 1.1\mu$W, $C_{\max} = 5$, $\delta = 0.2$s, $P_{\max} = 38$dBm, $\sigma_{\mathrm{R}}^2 = -70$dBm, $\sigma_k^2 = -80$dBm, $\varsigma = 1$, $P_C = 0.8$W, $a_\Omega = [0.085, 0.9 \times 10^6, 45]$, $\alpha_{\mathrm{MF}} = 10^4$, $\kappa = 0.9$, $\eta = 0.8$.

In Fig. 2, we show the geometric distributions of IUs and HAP, together with the real-time tracking results under different motion patterns. In both cases, the MEU starts from the same initial point with $\mathbf{u}^{\mathrm{E}} = [0.5, 2]^T$ m/s in Case 1 and $\mathbf{u}^{\mathrm{E}} = [3, 2]^T$ m/s in Case 2. Specifically, Case 1 (single-motion state) refers to a small process noise $\mathbf{z}_{pl}$ for MEU, whereas in Case 2 (multi-motion state) the MEU undergoes changes such as deceleration and steering, which correspond to considerably larger process noise. It can be observed that the real-time tracked trajectories generally match the actual curves in different motion cases, proving the good tracking performance of our proposed scheme.

To further study the WPT performance and gain more insight, we then follow the trajectory setup in Case 2 and consider three baseline schemes: 1)Upper Bound (UB): HAP has the perfect state $\mathbf{X}_l$, serving as an ideal case. 2)Time-Division Sensing (TDS) [15]: Each frame is split into two phases, where HAP senses $\mathbf{X}_l$ within $\alpha_t\delta$ and transmits within $(1-\alpha_t)\delta$, $\alpha_t = 0.3$. 3)Dedicated Device Sensing (DDS) [8]: HAP receives MEU's previous state $\mathbf{X}_{l-1}$ from the dedicated sensing device (e.g., UBW) and then predicts the current state, incurring additional power consumption $P_d = 1W$. As shown in Fig. 3, the MEU sensing error in each frame, defined as the instantaneous tracking MSEs with respect to $\mathbf{X}_l$ is presented. In 'PO design', sensing error is generated directly from the prediction state $\hat{\mathbf{X}}_{l|l-1}$ without ISAC modification. As can be observed, DDS scheme minimizes errors by leveraging additional sensing devices to capture and update the state vector of the previous frame accurately, unlike EKF-based schemes, which suffer from cumulative tracking errors. Nevertheless, the proposed scheme can reduce tracking errors compared to 'PO' by effective sensing. Interestingly, this improvement is particularly evident around the 25th and 50th frames, implying the limitations of relying solely on the state transition model to capture abrupt motion changes.

In Fig. 4, we depict the real-time WPT efficiency under different tracking schemes during the whole service time. As expected, the fluctuations reflect the MEU's motion state, as the RF signal strength decreases with increasing distance $d_{E,l}$, and the two peaks precisely correspond to the moments when MEU reaches its closest proximity to the HAP. The proposed scheme can approximate the 'UB' scheme in overall performance, with the gap attributed to sensing errors introduced by the predicted channel. In contrast, the other two schemes exhibit the lowest WPT values due to the additional time and power consumed by the sensing process. We illustrate the real-

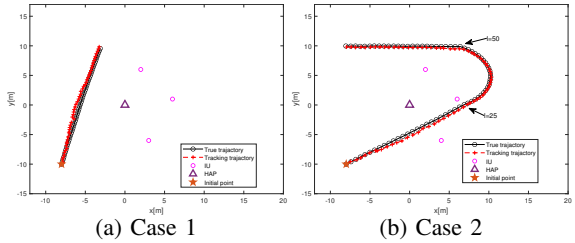

(a) Case 1 (b) Case 2

Fig. 2: Tracking trajectories by proposed scheme

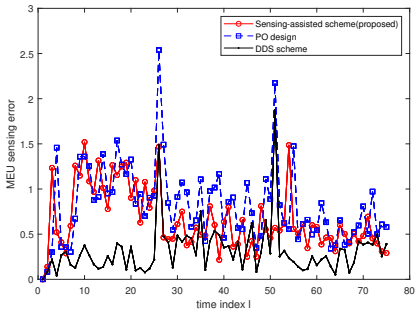

Fig. 3: MEU sensing error of Case 2 versus frame index l

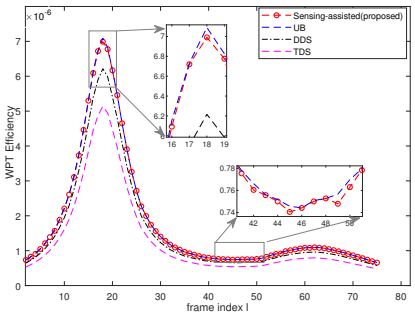

Fig. 4: Real-time WPT efficiency versus frame index l

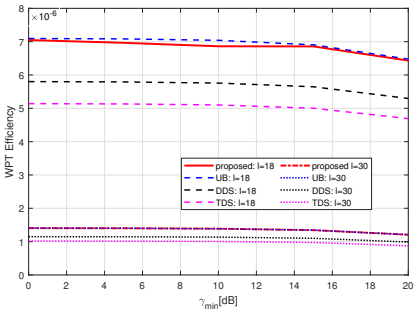

Fig. 5: Real-time WPT efficiency versus different SINR requirement

time WPT efficiency with respect to the SINR requirements $\gamma_{\min}$ in Fig. 5. The proposed scheme can closely approach the performance of the ideal 'UB' and consistently achieves higher WPT efficiency compared to DDS and TDS schemes. The WPT efficiency remains relatively stable initially, but as $\gamma_{\min}$ continues to increase, the WPT of all schemes gradually declines. This occurs because stricter communication requirements necessitate allocating more power to communication, thereby reducing the efficiency of power transfer, which also reveals the existence of a trade-off between communication and energy transfer.

V. Conclusion

In this letter, we proposed a novel dynamic sensing-assisted SWIPT system and investigated an EKF-based online beamforming framework to realize efficient power transfer. In particular, the beamforming design was formulated as a WPT efficiency maximization problem, subject to the specific QoS requirements for IUs and MEU. The original non-convex optimization problem is simplified and effectively solved by applying the Dinkelbach approach and SDR. Simulation results were provided to validate the proposed framework and performance gain over benchmark schemes.

References

[1] Y. Cui, F. Liu, X. Jing, and J. Mu, "Integrating sensing and communications for ubiquitous iot: Applications, trends, and challenges," *IEEE Network*, vol. 35, no. 5, pp. 158–167, 2021.

[2] T. D. Ponnimbaduge Perera, D. N. K. Jayakody, S. K. Sharma, S. Chatzinotas, and J. Li, "Simultaneous wireless information and power transfer (swipt): Recent advances and future challenges," *IEEE Communications Surveys & Tutorials*, vol. 20, no. 1, pp. 264–302, 2018.

[3] R. Ma, J. Tang, X. Zhang, K.-K. Wong, and J. A. Chambers, "Energy-efficiency optimization for mutual-coupling-aware wireless communication system based on ris-enhanced swipt," *IEEE Internet of Things Journal*, vol. 10, no. 22, pp. 19 399–19 414, 2023.

[4] J. Tang, Z. Peng, D. K. C. So, X. Zhang, K.-K. Wong, and J. A. Chambers, "Energy efficiency optimization for a multiuser irs-aided miso system with swipt," *IEEE Transactions on Communications*, vol. 71, no. 10, pp. 5950–5962, 2023.

[5] Q. Wu and R. Zhang, "Joint active and passive beamforming optimization for intelligent reflecting surface assisted swipt under qos constraints," *IEEE Journal on Selected Areas in Communications*, vol. 38, no. 8, pp. 1735–1748, 2020.

[6] J. Han, L. Li, X. Ma, X. Gao, Y. Mu, G. Liao, Z. J. Luo, and T. J. Cui, "Adaptively smart wireless power transfer using 2-bit programmable metasurface," *IEEE Transactions on Industrial Electronics*, vol. 69, no. 8, pp. 8524–8534, 2022.

[7] F. Liu, Y. Cui, C. Masouros, J. Xu, T. X. Han, Y. C. Eldar, and S. Buzzi, "Integrated sensing and communications: Toward dual-functional wireless networks for 6g and beyond," *IEEE Journal on Selected Areas in Communications*, vol. 40, no. 6, pp. 1728–1767, 2022.

[8] W. Mao, Y. Lu, G. Pan, and B. Ai, "Uav-assisted communications in sagin-isac: Mobile user tracking and robust beamforming," *IEEE Journal on Selected Areas in Communications*, pp. 1–1, 2024.

[9] K. Meng, Q. Wu, W. Chen, E. Paolini, and E. Matricardi, "Intelligent surface empowered sensing and communication: A novel mutual assistance design," *IEEE Communications Letters*, vol. 27, no. 8, pp. 2212–2216, 2023.

[10] Z. Wei, F. Liu, C. Liu, Z. Yang, D. W. K. Ng, and R. Schober, "Integrated sensing, navigation, and communication for secure uav networks with a mobile eavesdropper," *IEEE Transactions on Wireless Communications*, vol. 23, no. 7, pp. 7060–7078, 2024.

[11] S. Ma, H. Sheng, R. Yang, H. Li, Y. Wu, C. Shen, N. Al-Dhahir, and S. Li, "Covert beamforming design for integrated radar sensing and communication systems," *IEEE Transactions on Wireless Communications*, vol. 22, no. 1, pp. 718–731, 2023.

[12] Y. Chen, H. Hua, J. Xu, and D. W. K. Ng, "Isac meets swipt: Multi-functional wireless systems integrating sensing, communication, and powering," *IEEE Transactions on Wireless Communications*, vol. 23, no. 8, pp. 8264–8280, 2024.

[13] Z. Zhou, X. Li, G. Zhu, J. Xu, K. Huang, and S. Cui, "Integrating sensing, communication, and power transfer: Multiuser beamforming design," *IEEE Journal on Selected Areas in Communications*, vol. 42, no. 9, pp. 2228–2242, 2024.

[14] Y. Yang, H. Gao, X. Yang, R. Cao, and Y. Fan, "Joint beamforming for ris-assisted integrated communication, sensing and power transfer systems," *IEEE Wireless Communications Letters*, vol. 13, no. 2, pp. 288–292, 2024.

[15] Y. Xu, D. Xu, and S. Song, "Sensing-assisted robust swipt for mobile energy harvesting receivers," *arXiv preprint arXiv:2402.09976*, 2024.

[16] F. Liu, W. Yuan, C. Masouros, and J. Yuan, "Radar-assisted predictive beamforming for vehicular links: Communication served by sensing," *IEEE Transactions on Wireless Communications*, vol. 19, no. 11, pp. 7704–7719, 2020.

[17] S. M. Kay, "Fundamentals of statistical signal processing: Estimation theory," 1993.

[18] J. Yan, H. Liu, B. Jiu, B. Chen, Z. Liu, and Z. Bao, "Simultaneous multibeam resource allocation scheme for multiple target tracking," *IEEE Transactions on Signal Processing*, vol. 63, no. 12, pp. 3110–3122, 2015.

[19] W. Dinkelbach, "On nonlinear fractional programming," *Management science*, vol. 13, no. 7, pp. 492–498, 1967.

[20] Z.-q. Luo, W.-k. Ma, A. M.-c. So, Y. Ye, and S. Zhang, "Semidefinite relaxation of quadratic optimization problems," *IEEE Signal Processing Magazine*, vol. 27, no. 3, pp. 20–34, 2010.

[21] S. Boyd and L. Vandenberghe, *Convex optimization*. Cambridge university press, 2004.

[22] Y. Huang, "Challenges and opportunities of sub-6 ghz integrated sensing and communications for 5g-advanced and beyond," *Chinese Journal of Electronics*, vol. 33, no. 2, p. 323, 2024. [Online]. Available: https://cje.ejournal.org.cn/en/article/doi/10.23919/cje.2023.00.251

[23] T. Jiang, Y. Zhang, W. Ma, M. Peng, Y. Peng, M. Feng, and G. Liu, "Backscatter communication meets practical battery-free internet of things: A survey and outlook," *IEEE Communications Surveys & Tutorials*, vol. 25, no. 3, pp. 2021–2051, 2023.